

Non-HAP CAM-A ALG-006746 and ALG-006780 induce rapid HBsAg reductions in AAV-HBV mice and have favorable pharmacokinetic profiles

Hannah Vanrusselt¹, Jordi Verheyen¹, Kusum Gupta², Lars Degrauwe¹, Cheng Liu², Abel Acosta Sanchez³, Mélanie Bollier³, Jean-Boris Nshimyumuremyi³, Benjamin Verburgh³, Clovis Peter³, Qingling Zhang², Lawrence M. Blatt², Leonid Beigelman², Julian A. Symons², Sushmita Chanda², David B. Smith², Andreas Jekle², Sandrine Vendeville¹, David McGowan¹, Yannick Debing¹

¹ Aligos Belgium BV, Leuven, Belgium; ² Aligos Therapeutics, Inc., South San Francisco, CA; ³ Novalix, Leuven, Belgium

Background and aims

Hepatitis B virus (HBV) capsid assembly is an attractive target for the treatment of chronic hepatitis B (CHB).¹ Class A capsid assembly modulators (CAM-A) induce HBV core protein (Hbc) aggregation and sustained HBsAg reduction in CHB mouse models.² RG7907 (linvencorvir) and GLS4 (morphothiadin) are well-characterized heteroaryldihydropyrimidine (HAP) CAM-A. We recently presented data on the first non-HAP CAM-A with sustained in vivo HBsAg declines.³ Here we present two novel non-HAP CAM-A that demonstrate rapid HBsAg reductions in AAV-HBV mice and favorable pharmacokinetic (PK) profiles.

ALG-006746 and ALG-006780 are potent HBV DNA inhibitors

ALG-006746 and ALG-006780 potently inhibited HBV DNA production in HepG2.117 cells with EC₅₀ / EC₉₀ values of 10.6 / 45.0 nM and 7.76 / 31.6 nM respectively. Inclusion of 40% human serum resulted in modest 2.3- and 1.7-fold shifts in antiviral activity, respectively.

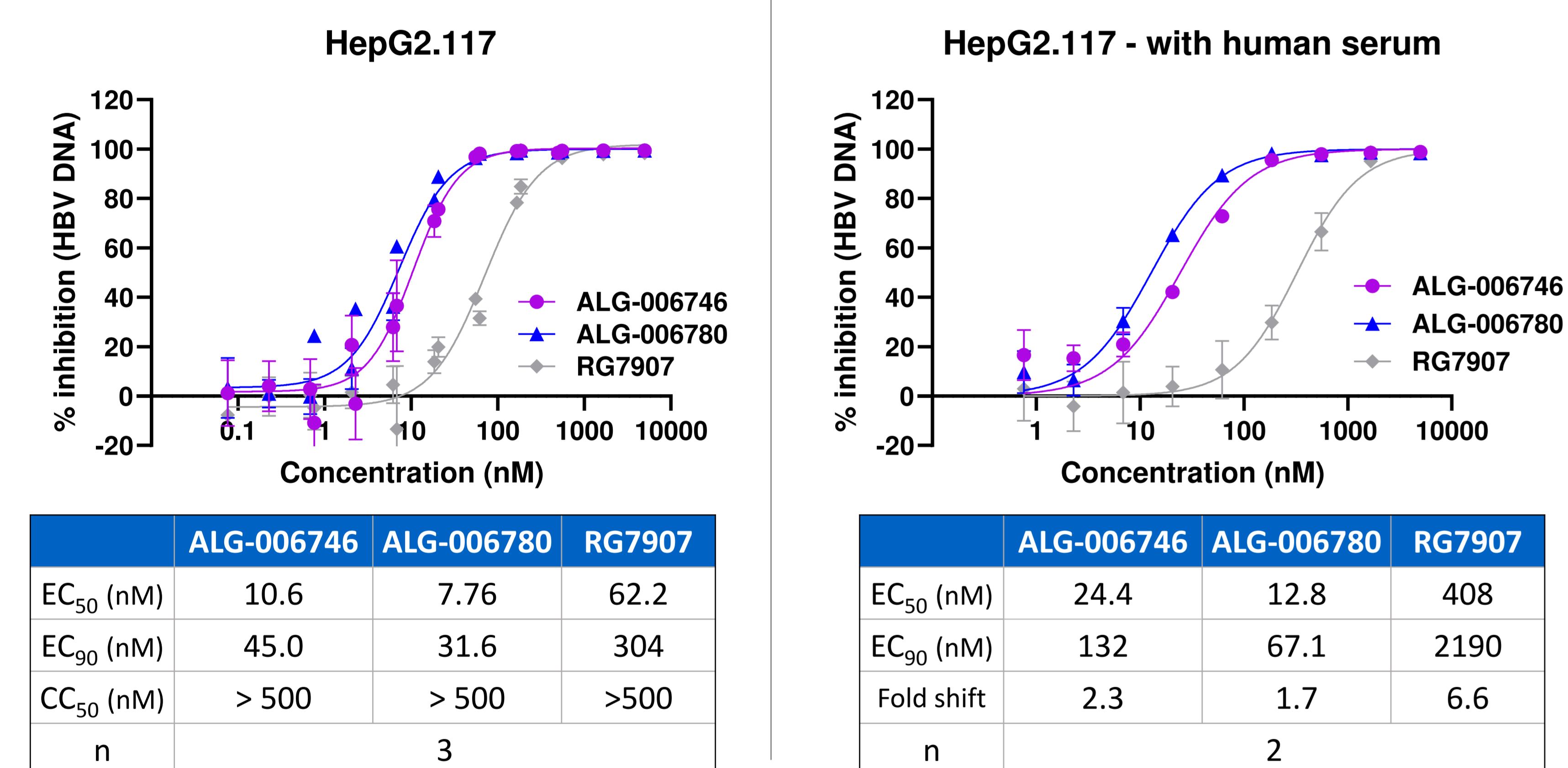


Figure 1 – Left: Dose-response curves for inhibition of HBV DNA replication in HepG2.117 cells. Curves and values represent mean ± SEM from 3 independent experiments. **Right:** Dose-response curves for inhibition of HBV DNA replication in HepG2.117 cells in the presence of 40% human serum. Curves and values represent mean ± SEM from 2 independent experiments.

ALG-006746 and ALG-006780 are potent inhibitors of RNA encapsidation and cccDNA establishment in HBV-infected primary human hepatocytes

When ALG-006746 or ALG-006780 were added to an established HBV infection in PHH (5 days post infection), HBV DNA production was blocked efficiently. In addition, cccDNA formation was strongly inhibited when compound was added at the time of infection, as evidenced by reductions in extracellular HBsAg and HBeAg, and intracellular HBV RNA. In contrast, RG7907 was much less effective in preventing cccDNA formation, not reaching full inhibition, even at very high concentrations.

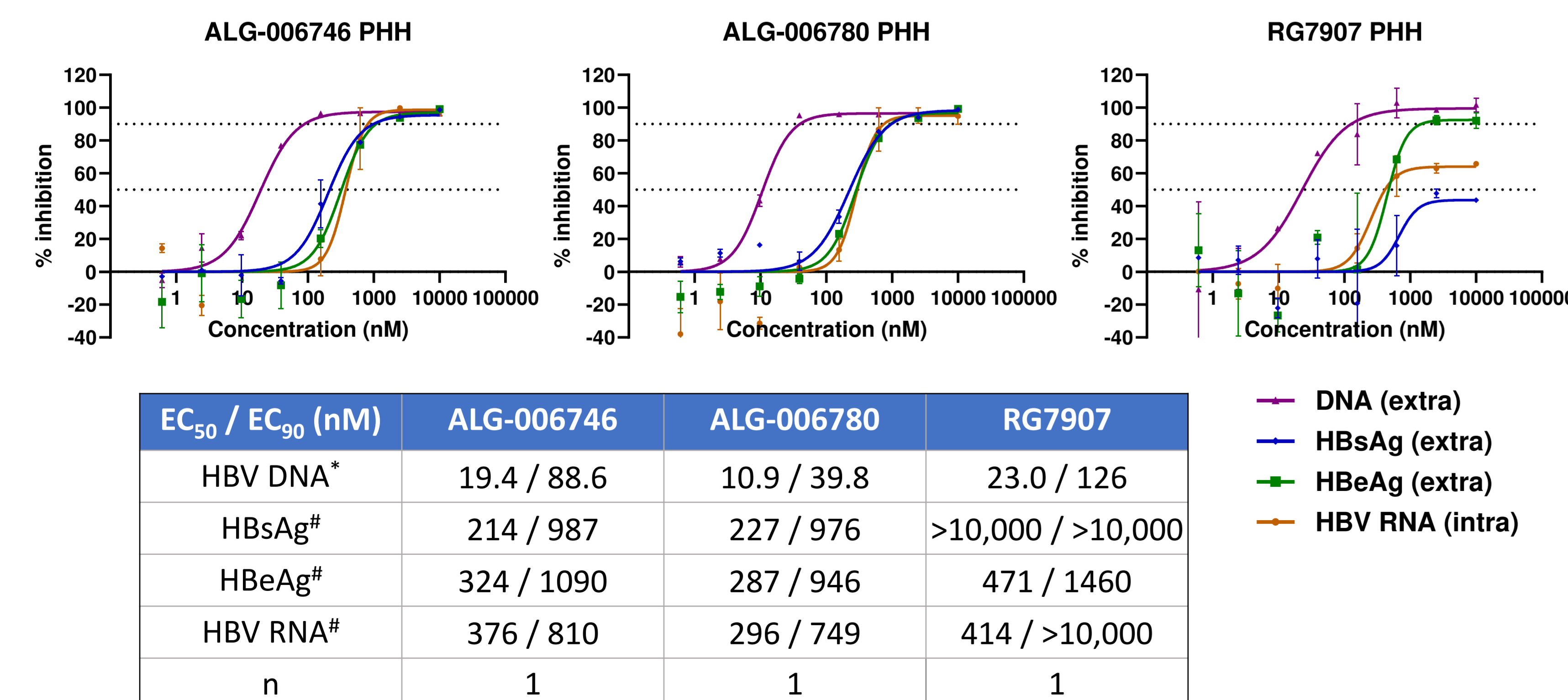


Figure 2: Dose-response curves for ALG-006746-, ALG-006780- and RG7907-induced inhibition of HBV DNA, RNA, HBsAg and HBeAg production in HBV-infected primary human hepatocytes. Values represent mean ± SEM from 1 experiment. * Compound added 5 days after infection; # compound added at time of infection.

Methods

HBV DNA antiviral activity was determined in HepG2.117 cells, which contain a stably integrated genotype D HBV genome, using quantitative PCR, with and without 40% human serum.⁴ Effects on cccDNA establishment were assessed in HBV-infected primary human hepatocytes (PHH). Further characterization was performed using electron microscopy visualization and immunofluorescent Hbc staining. Hbc-dependent CAM-A-induced cell death (CCD) was assessed in Hbc-expressing cells.² PK properties were evaluated in rat, dog and cynomolgus monkey; in vivo antiviral efficacy was assessed in the adeno-associated virus (AAV)-HBV mouse model.⁵

ALG-006746 and ALG-006780 induce formation of aberrant particles in vitro and small nuclear Hbc aggregates in HepG2.117 cells

Class A CAMs induce the formation of aberrant viral particles when incubated with recombinant Hbc. This could clearly be observed for ALG-006746 and ALG-006780, similar to reference CAM-A GLS4. In a cellular setting, this leads to the formation of nuclear Hbc spots, representing compound-induced Hbc aggregates.^{2,3,6} Such spots were also observed when HepG2.117 cells were treated with ALG-006746 and ALG-006780, although a different phenotype was observed compared to RG7907: spots were more numerous but smaller in size, confirming their CAM-A “tiny” (CAM-A_t) subtype.³ Quantification of the total spot area normalized to cell number and relative to RG7907 at 10 μM allowed the determination of EC₅₀ values of 148 and 320 nM for ALG-006746 and ALG-006780, respectively, making them 4-7x more potent than RG7907 (EC₅₀ of 1170 nM) in inducing Hbc spots.

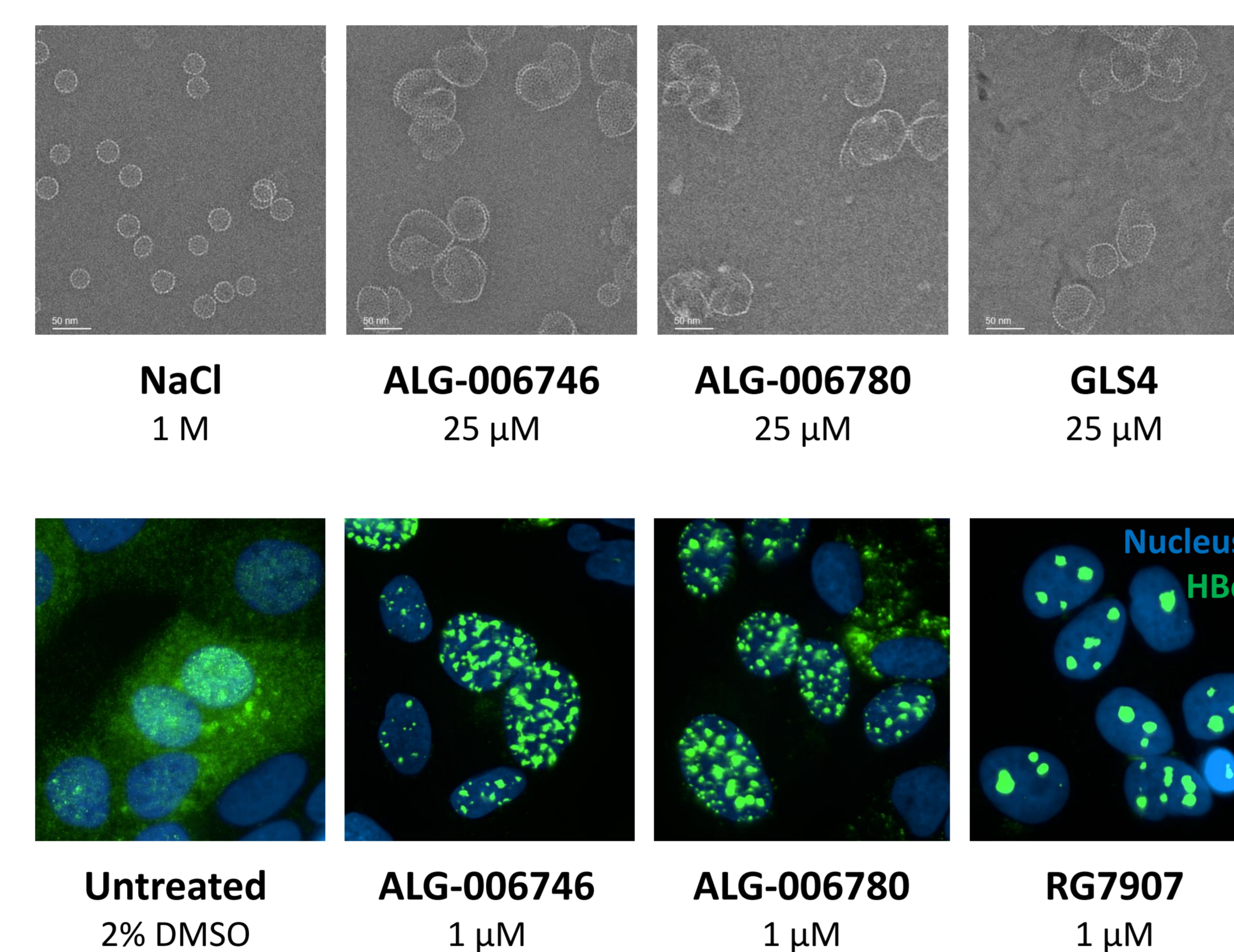


Figure 3: Electron microscopy images of Hbc incubated with NaCl (1 M) – resulting in empty regular capsids, or ALG-006746, ALG-006780 or GLS4 (25 μM) – resulting in aberrant capsids, confirming their CAM-A nature.

Figure 4 – Left: Immunofluorescent staining of HepG2.117 cells for Hbc; CAM-A induce loss of cytoplasmic Hbc and formation of nuclear Hbc aggregates with different phenotypes for RG7907 vs ALG-006746 and ALG-006780. **Right:** Quantification of spotting by automated image analysis (total spot area normalized to cell number and relative to RG7907 at 10 μM). Curves and values represent mean ± SEM from 2 independent experiments.

ALG-006746 and ALG-006780 induce Hbc-dependent cell death

We recently showed that CAM-A-induced Hbc-dependent cell death (CCD) can be reproduced in Hbc-expressing cells.² To confirm that ALG-006746 and ALG-006780 also induce CCD, HepG2-NTCP cells overexpressing HA-Hbc or HA-HBsAg were treated with different compound concentrations for 14 days and cell viability was assessed. Similar to RG7907, both ALG-006746 and ALG-006780 decreased cell viability in a dose-dependent fashion, in Hbc-overexpressing cells, but not in HBsAg-overexpressing cells, confirming the Hbc-dependency of this phenomenon.

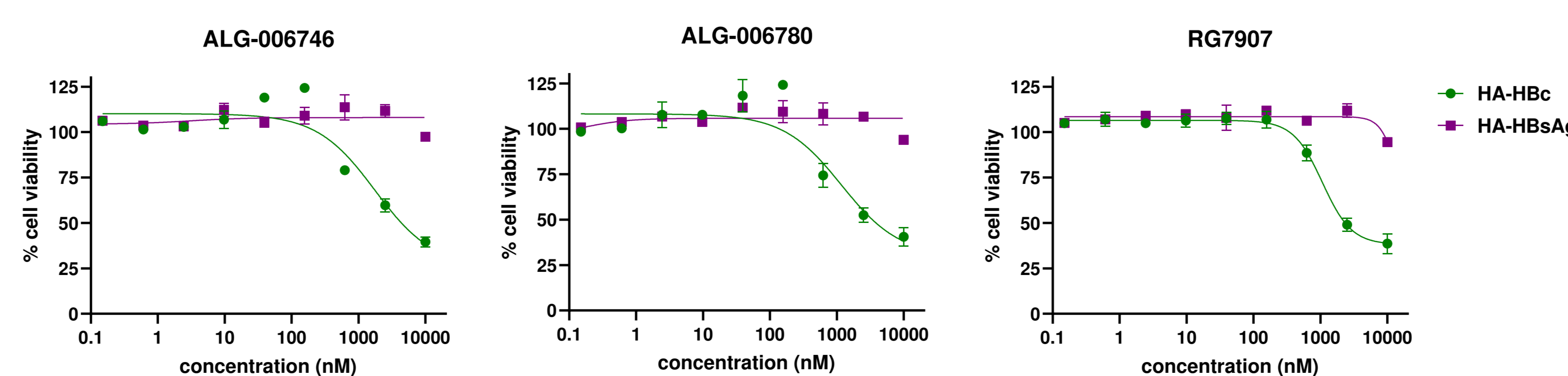
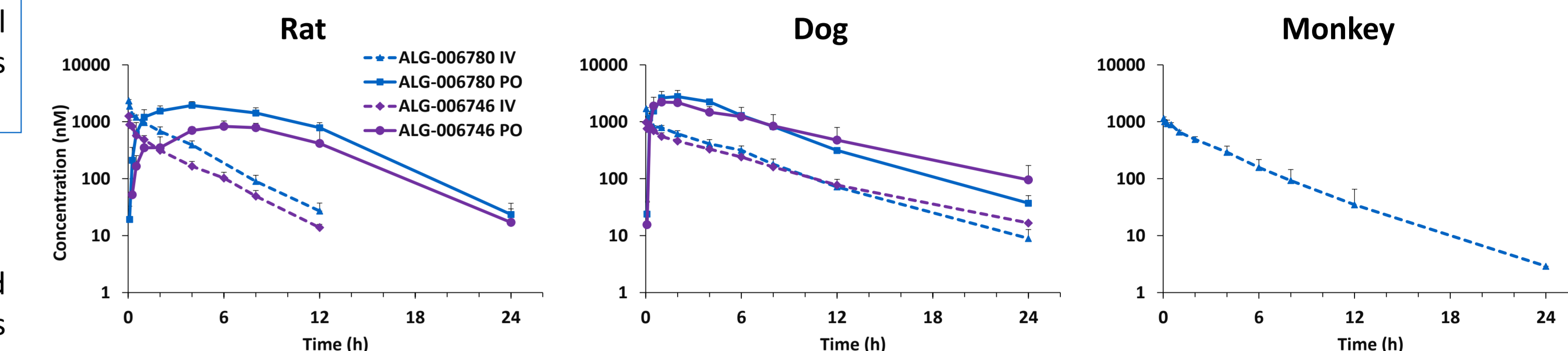


Figure 5: Dose-response curves for ALG-006746-, ALG-006780 and RG7907-induced CCD HA-Hbc- or HA-HBsAg-overexpressing HepG2-NTCP cells. Values represent mean ± SEM from 1 experiment.

ALG-006746 and ALG-006780 show favorable PK profiles

Both compounds showed low to moderate plasma clearance and moderate volume of distribution in three different species. Following a single oral administration of each compound in rat and dog, good bioavailability (79-91%) was achieved.



	Rat		Dog		Monkey
Plasma PK Parameters	ALG-006746	ALG-006780	ALG-006746	ALG-006780	ALG-006780
IV Dose (mg/kg)	2 (fasted)	1 (fasted)	1 (fasted)	1 (fasted)	1 (fasted)
T _{1/2} (h)	2.12	2.25	4.58	3.50	2.70
Vd _{ss} (L/kg)	4.29	2.17	2.34	1.61	1.71
Cl (mL/min/kg)	24.3	12.3	6.36	5.62	8.29
PO Dose (mg/kg)	10 (fed)	10 (fed)	5 (fasted)	5 (fasted)	
T _{1/2} (h)	2.62	3.35	4.83	4.20	
C _{max} (nM)	893	1969	2407	2811	
AUC ₀₋₂₄ (h·nM)	8476	18982	17346	18340	
F%	81.6	89.3	91.1	79.1	

Figure 6 – Top: ALG-006746 and ALG-006780 plasma profiles following single IV or PO administration. **Bottom:** Plasma PK parameters for the different species. Values represent mean from 3 animals per species.

ALG-006746 and ALG-006780 induce rapid HBsAg reduction in vivo with minimal ALT increase

The AAV-HBV model was used to assess the efficacy of ALG-006746 and ALG-006780 in vivo.⁵ ALG-006746 at 15 mg/kg/dose BID and ALG-006780 at 10 mg/kg/dose BID both resulted in a multiphasic reduction in HBV DNA, with a 6 log₁₀ IU/mL reduction after 84 days of treatment. For ALG-006746 a significant decrease in serum HBsAg levels was observed with a 1.8 log₁₀ IU/mL reduction with paced kinetics, with a short ALT flare. Similar to RG7907 at 20 mg/kg/dose QD, ALG-006780 induced a rapid decrease in HBsAg level with a 2 log₁₀ IU/mL reduction, with a similar small ALT spike. Significant decreases in HBeAg levels were also noted but less pronounced compared to HBsAg decline.

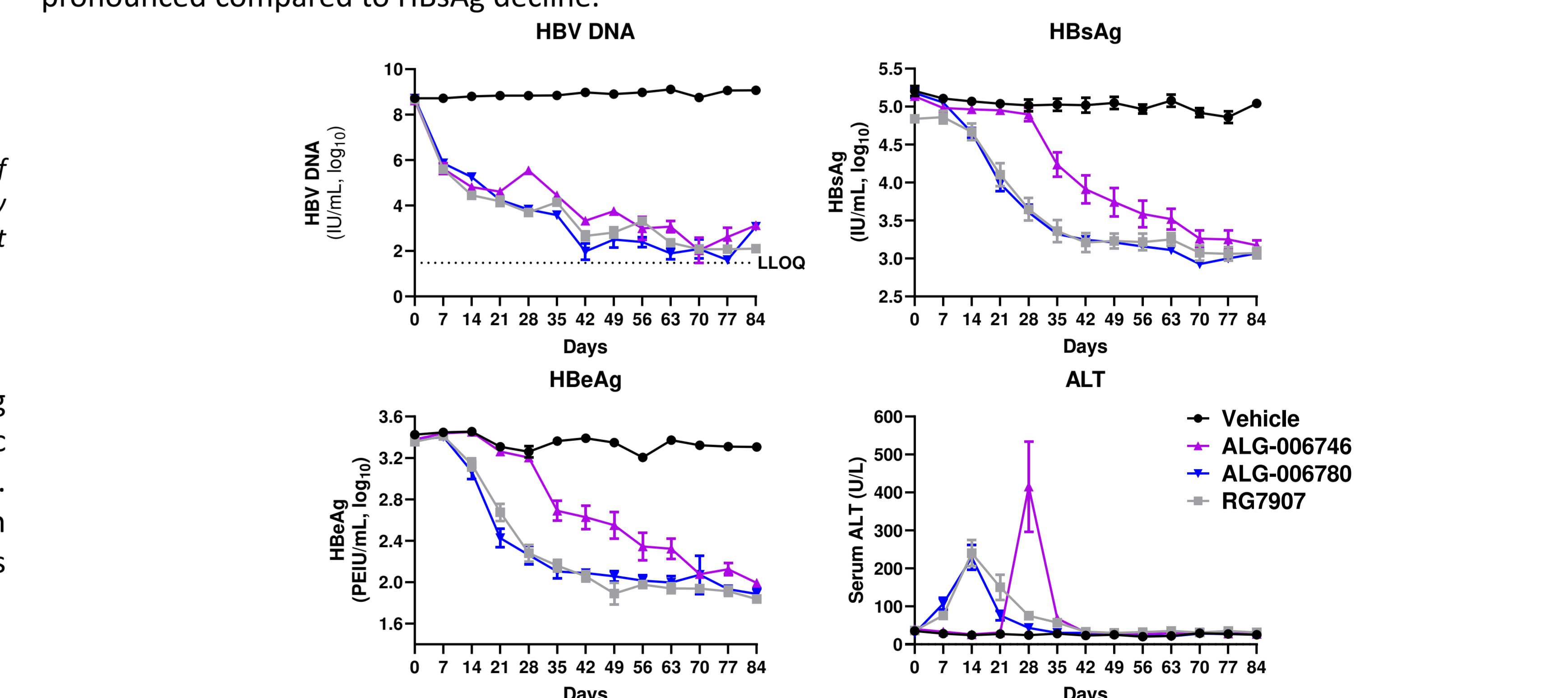


Figure 7: Kinetics of serum levels of HBV DNA, HBsAg, HBeAg and ALT in AAV-HBV mice during treatment, with statistically significant declines for HBV DNA, HBsAg and HBeAg. Values represent mean ± SEM for 4 animals per group.

Conclusions
With rapid in vivo HBsAg declines and favorable PK profiles, ALG-006746 and ALG-006780 are promising CAM-A candidates for further development that are clearly differentiated from RG7907.

References

[1] Taverniti et al 2022 J Clin Med, 11: 1349. [2] Kum et al 2023 Hepatology, 78: 1252-65. [3] Vanrusselt et al 2023 J Virol, 97: e0072223. [4] Sun & Nassal 2006 J Hepatol, 45: 636-45. [5] Yang et al 2014 Cell Mol Immunol, 11: 71-8. [6] Corcuera et al 2018 Antiviral Res, 158: 135-42.

Financial disclosures

All authors are or were directly or indirectly employed by Aligos Therapeutics, Inc. and may own stock.